

Establishment of probabilistic radar quantitative precipitation estimates in the Cévennes region



"Pont du Gard" during the 8-9 September 2002 catastrophic event.

Savina Partheni^a
LTHE Grenoble

^aMaster 2 Research HydroHazards, University Joseph Fourier, 38000 Grenoble, France

Abstract

Radar quantitative precipitation estimates (QPE) have been assessed using reference values established by a geostatistical approach in the context of flash-flood prediction in the Cévennes region France. The reference values were estimated from rain gauge data using the Block Kriging technique and the reference meshes were selected on the basis of the Kriging estimation variance. An empirical radar error model was built by computing the spatial means and the covariance matrix of the errors, as well as their autocorrelation function. In addition, the conditional statistical distributions of the errors were established with respect to several variables and factors (rain amount, radar range, mountain versus plain region of the domain of interest) using the “generalized additive models for location, scale and shape” (GAMLSS) approach. The conditional bias of the errors presents a complex structure that depends on the space-time scales and the considered geographical sub-domains, while the standard deviation of the errors has a more homogeneous behaviour with a linear increase as a function of the rain amount. The probabilistic QPE generator proposed by Germann et al. (2009) was implemented for the 1-hour time step and for hydrological meshes of about 100 km², which are space-time scales relevant for the flash-flood prediction in the Cévennes region. Several improvements of the original approach were proposed with, in particular, the conditioning of the errors for the observed dependency on the rain amount. The way the errors propagate in the hydrological modelling system remains to be studied with the n-TOPMODELS model.

Περίληψη

Ποσοτικές εκτιμήσεις βροχόπτωσης από ραντάρ (ΠΕΒ) έχουν αξιολογηθεί χρησιμοποιώντας έγκυρες τιμές αναφοράς μέσω γεωστατιστικής προσέγγισης στα πλαίσια της πρόβλεψης πλημμυρών για την περιοχή Cévennes στην Γαλλία. Οι τιμές αναφοράς υπολογίστηκαν με βάση βροχομετρικά στοιχεία και την τεχνική Block – Kriging, ενώ τα υδρολογικά πλέγματα αναφοράς, επιλέχθηκαν βάσει την εκτίμηση της διακύμανσης Kriging. Ένα εμπειρικό μοντέλο σφάλματος ραντάρ δημιουργήθηκε από τον υπολογισμό του χωρικών μέσων και τον πίνακα συνδιακύμανσης των σφαλμάτων, καθώς και τον βαθμό αυτοσυσχετίσής τους. Επιπλέον, η υπό όρους στατιστικές κατανομές των σφαλμάτων συστάθηκαν σε σχέση με πολλές μεταβλητές και παράγοντες (ύψος βροχής, εύρος ραντάρ, βουνό έναντι πεδιάδας της περιοχής ενδιαφέροντος) χρησιμοποιώντας την προσέγγιση “Γενικευμένα μοντέλα για τοποθεσία, μέγεθος και σχήμα» (GAMLSS). Η υπό όρους αμεροληψία από τα σφάλματα, παρουσιάζει μια πολύπλοκη δομή που εξαρτάται από χωροχρονικές κλίμακες και από γεωγραφικούς υπο-τομείς, ενώ η τυπική απόκλιση των σφαλμάτων έχει μια πιο ομοιογενή συμπεριφορά με γραμμική αύξηση σε συνάρτηση με το ύψος της βροχής. Η πιθανολογική εκτίμηση βροχόπτωσης που προτείνει ο Germann et al. (2009) τέθηκε σε εφαρμογή για χρονικό βήμα μιας ώρας και για υδρολογικά πλέγματα των 100 km², τα οποία καθιστούν χωροχρονικές κλίμακες για την πρόβλεψη πλημμυρών στην περιοχή Cévennes. Αρκετές βελτιώσεις της αρχικής προσέγγισης προτάθηκαν, μεταξύ άλλων, την υπό όρους προετοιμασία των σφαλμάτων που παρατηρήθηκαν σχετικά με την εξάρτηση από το ύψος βροχής. Ο τρόπος που τα σφάλματα διαδίδονται στο υδρολογικό σύστημα μοντελοποίησης μένει να μελετηθεί με το n-TOPMODELS μοντέλο.

Résumé

Des estimations de précipitations quantitatives à partir de radar (QPE) ont été élaborées en utilisant des valeurs de références établies par une approche géostatistique dans un contexte de prévision de crue éclairée dans la région des Cévennes en France.

Les valeurs de références ont été estimées à partir de données de pluviométriques à l'aide de la technique de krigeage par bloc et les réseaux hydrographiques ont été sélectionnés sur la base du krigeage de l'estimation de la variance. Un modèle empirique d'erreur radar a été construit en calculant les moyennes spatiales et la matrice de covariance des erreurs, ainsi que les fonctions d'autocorrélations. De plus, la distribution statistique conditionnelle des erreurs a été établie en respect de plusieurs variables et facteurs (quantité de pluie, portée du radar, les zones de montagnes contre les zones de plaines de la région d'intérêt) en utilisant l'approche du modèle additif généralisé pour le lieu, l'échelle et la forme (GAMLSS). Le biais conditionnel des erreurs présente une structure complexe qui dépend de l'échelle spatio-temporelle et du sous-domaine géographique considéré, alors que l'écart-type de l'erreur a un comportement plus homogène avec une augmentation linéaire en fonction de la quantité de pluie. La génération probabilistique de QPE proposée par Germann et al. (2009) a été implémentée au pas de temps d'une heure pour des réseaux hydrographiques de l'ordre de 100 km², qui sont à l'échelle spatio-temporelle représentative pour la prévision de crue éclairée dans la région des Cévennes. Plusieurs améliorations de l'approche originale ont été proposées avec, en particulier, le conditionnement des erreurs sur la dépendance des quantités de pluies observées. La manière dont les erreurs se propagent dans un modèle hydrologique reste à étudier avec le modèle n-TOPMODEL.

1. Introduction

A key component in many hydro meteorological forecasting systems is the rainfall – runoff hydrological models, which aims to translate observations and forecasts of rainfall into estimates for river flows. Distributed hydrological models (Ogden *et al.* 2001), although more complex compared to lumped models, provide additional insight on hydrological conditions, such as soil moisture and stream flow, at locations without existing flow observations (Carpenter and Georgakakos, 2003). For the development and application of hydrological models a widespread implementation of weather radar has been established, in order to advantage the high spatial and temporal resolution of the precipitation estimates from the radars. However, it is crucial to consider the significant uncertainties which exist in radar rainfall estimates obtained from radar reflectivity, in hydrological parameters derived from available databases and in the model structure as well. This complexity leads to high spatial heterogeneity, forcing us to consider the error sources in radar rainfall measurements, in order to improve the quantitative precipitation estimation (QPE), assess the QPE errors and how they propagate in the hydrological modeling system.

Considering the context of flash floods, several European projects have been established (HYDRATE, FLOODsite), aimed to improve the flash flood forecasting by developing a coherent set of technologies for effective early warning systems. A crucial point at these efforts is the quantitative precipitation estimation, since the causative rain events may develop over very short space and time scales (Krajewski and Smith, 2002; Creutin and Borga, 2003). The rainfall measurements from operational rain gauges networks are often available at best at the

hourly time scale with often too low spatial resolutions. So in order to describe the rainfall – runoff dynamics at hourly or over shorter time steps, ground-based weather radar data, are becoming widely available and used in hydrological forecasting.

The assessment of the radar data on hydrological modeling is complex since it depends on the system design (radar location and operating protocol) and on the data processing (Austin, 1987; Joss and Waldvogel, 1990; Yuter, 2002). Some of the main problems that we have to deal with are, the beam smoothing and post-detection integration (Zawadzki, 1982), the beam shielding and the vertical profiles of reflectivity (Joss and Waldvogel, 1990; Kitchen, 1995; Joss and Lee, 1995; Pellarin *et al.*, 2002; German and Joss, 2002; Bellon *et al.*, 2007), variability in raindrop size distributions and related uncertainty in the relation between reflectivity and rain rate (Joss and Gori, 1978; Lee and Zawadzki, 2005).

Due to these uncertainties it is important to understand the processes and characterize the error structure of radar precipitation estimates. A physical approach would be to examine all sources of errors separately and to evaluate their cumulative effects. Several studies have been conducted based on this physical approach (Jordan *et al.*, 2003; Pellarin *et al.*, 2002; Berenguer and Zawadzki 2008), which aimed to go a step closer to the understanding of the error structure of QPEs. However the combined effects of the errors and the implementation of radar data processing algorithms (Delrieu *et al.*, 2009; Tabary, 2007; Tabary *et al.*, 2007) limit the relevance of this physical approach to error analysis and make it hardly tractable in practice. Therefore, in order to characterize the overall uncertainty, another common approach is to evaluate radar QPE accuracy with respect to an external reference. Dense raingauge networks are generally used for this purpose, although the raingauge measurements are known to suffer from lack of spatial representativity, especially for short integration time steps. In spite of significant progress, the residual errors between radar and reference values are still large and it is important to take them into account, in order to assess accurate flood forecasts. Additionally, it is expected that uncertainties in rainfall input data will be modified into predictions from hydrologic models (Morin *et al.* 2005; Hossain *et al.* 2004; Borga 2002; Sharif *et al.* 2002; Winchell *et al.* 1998; Vieux and Bedient 1998; Pessoa *et al.* 1993). Therefore, accurate characterization of radar rainfall errors and their spatial and temporal structure, as well as the induced uncertainties in hydrological modeling is very important. The ultimate objective of this work is to provide a statistical framework for producing probabilistic space-time series of rainfall based on the QPE error model that would be used to assess the impact of rainfall uncertainties upon hydrological modeling at regional scale.

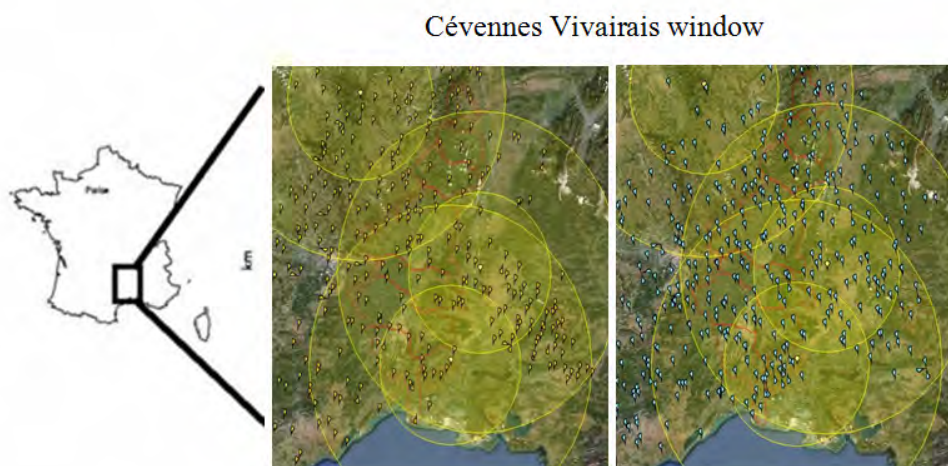
In order to express the residual uncertainties in radar estimates, a promising effort would be the generation of an ensemble of precipitation fields (e.g. Krajewski and Georgakakos, 1985). Each member on the ensemble is a possible realization and knowledge on the radar error structure (Germann *et al.*, 2006a; Lee *et al.*, 2007). The deterministic radar precipitation field is perturbed by a stochastic component, which has the correct space – time covariance structure as defined by the radar error covariance matrix (German *et al.*, 2009).

A step forward is proposed in the present work in order to derive QPE ensembles for the Cévennes–Vivairais Mediterranean Hydro-meteorological Observatory window (CVMHO) and to study the propagation of the error structure of the simulated discharges as a function of the probabilistic QPE characteristics. Our work starts with the Germann *et al.* (2009) approach and one of our main challenges was to account for the dependence of the residuals on the rain rate evidenced in previous works (Kirstetter *et al.* 2010; Delrieu *et al.* 2012). For the hydrological simulations the n-Topmodel codes which were developed and used in the LTHE laboratory (Pellarin *et al.* 2002; Le Lay and Saulnier 2009; Bonnifait *et al.* 2009), were implemented on a number of upstream tributaries of the main Cévennes rivers (Ardèche, Cèze, Gardons and Vidourle).

A detailed description of CVMHO datasets used in the present study is presented in section 2. The radar error model with the *spatial and temporal structure* is analyzed in section 3, while we present the generation of the QPE ensemble under two conditionings in section 4. The implementation of the hydrological model is described in Section 5, and this study ends up with the conclusions in section 6.

2. Case study basins and dataset

The south-eastern ridge of the Massif-Central in France, prone to flash-flooding, is included in the Cévennes Vivarais Mediterranean Hydrometeorological Observatory (CVMHO) window, covering a region of 200 x 160 km². This area is characterized by a dense rain gauge network with measurements for hourly and daily time steps. Moreover, the installation of two weather radar systems, the Nimes S-band and Bollène 2002, provides satisfactory coverage for the most of the catchments in the southern part of the region (Figure 1). The observed rain events that were selected for this study occurred on the 8/09/2002, 27/09/2007, 19/10/2008 and 31/10/2008 and concern the four main watersheds prone to flash flood (Ardèche, Cèze, Gardons and Vidourle rivers) (Figure 2). These rain events produced major traffic disturbances leading to lives and property casualties. The most severe event was that on 8/09/2002, which is one of the 23 severe flash – flood cases occurring in Spain, France, Italy, Austria, Greece and UK that were documented within the HY-DRATE project (Kirstetter et al, 2010).



Source: (<http://www.ohmcv.fr/>)

Figure 1: CVMHO observation window. Location and 50-km range markers of the Bollène, Nimes, Sembadel weather radar with the available rain gauge system at hourly (left) and daily (right) time step superimposed on the orography of the Cévennes – Vivarais region. The main watersheds are also displayed in the graph with the red line.

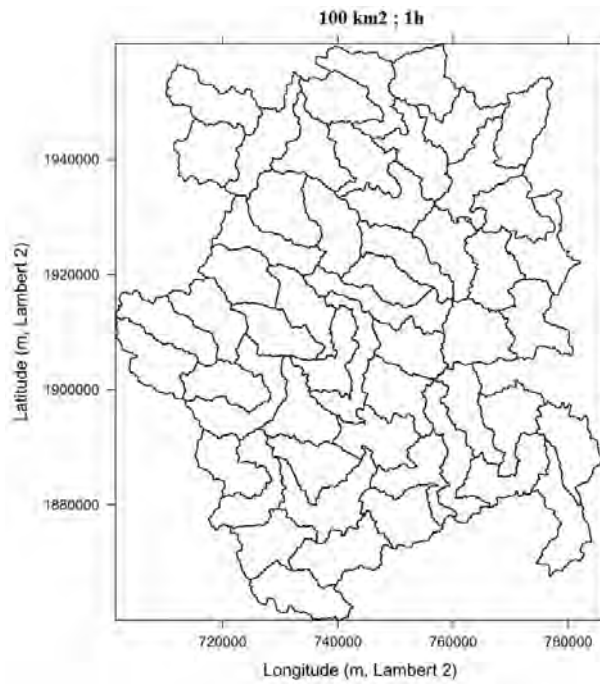


Source: (<http://www.ohmcv.fr/>)

Figure 2: The four main watersheds (Ardèche River, 242km²; Cèze River, 1054km²; Gard River, 1913km²; Vidourle River, 621km²) delimited with the red solid lines. The main rivers are also displayed in the graph with the blue solid line.

Regarding radar QPE, we used the products obtained from a radar processing system, called *Traitements Régionalisés et Adaptatifs de Données Radar pour l'Hydrologie* (Regionalized and Adaptive Radar Data Processing for Hydrological Applications) (Delrieu et al, 2009). This development radar processing system, initiated in 2002 at LTHE, as part of the activities of the CVMHO, includes algorithms which relies on 1) a clutter identification technique based on the pulse-to-pulse variability of reflectivity Z for noncoherent radar, 2) a coupled procedure for determining a rain partition between convective and widespread rainfall and the associated normalized vertical profiles of reflectivity, and 3) a method for calculating reflectivity at ground level from reflectivities measured aloft. Several data - processing strategies, including non-adaptive, time-adaptive, and space-time-adaptive variants were assessed (Delrieu et al, 2009). In the following we focus on the results of the space-time adaptive strategy. Moreover, effective Z - R relationships were optimized for each event separately using the procedure proposed by Bouilloud et al. (2010) in order to reduce the bias and the conditional bias of the radar QPEs.

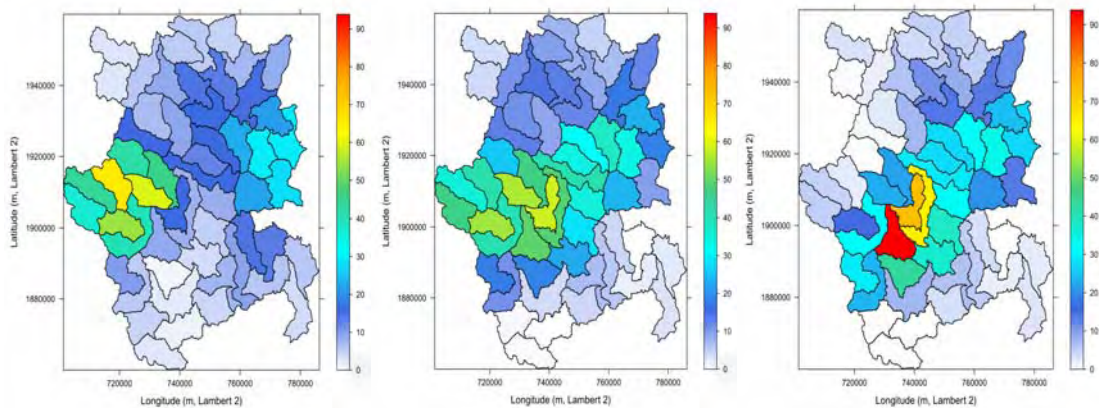
In this work we consider the spatial discretization of the four of the main Cévennes watershed into hydrological meshes of 100 km² (Figure 3). The study was based on matrix computation of kxi entries, for a k number of meshes and i the number of the time steps. The 08/09/2002 event was the more severe, with total rain amounts reaching locally 700mm in 28 h. The rainfall affected all of the four main watersheds. The characteristics of that flood event was controlled by the trajectory of the convective part of a mesoscale convective system (MCS), which remained stationary over CVMHO window for 28 h being responsible for the exceptional magnitude of the flood at this scale (Bonnifait et al, 2009). The 29/10/2007 event was a more localized event, with the excessive rain rate being localized in the downstream tributaries of the Vidourle and Gardons watersheds, while the 19/10/2008 and 31/10/2008 events, and were intense rain events affecting the upstream parts of the Ardèche, Cèze and Vidourle watersheds (Figure 4).



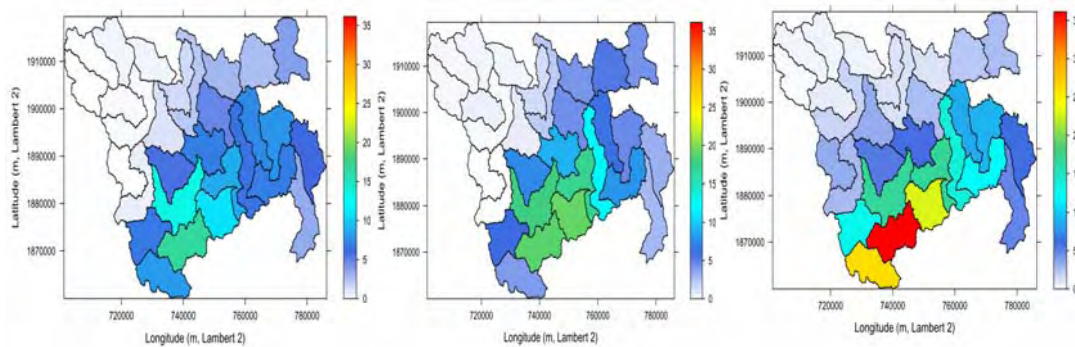
Source: (Kirstetter et al, 2010)

Figure 3: Spatial discretization of the four of the main Cèvennes watersheds (Ardèche River, 2500km²; Cèze River, 1054km²; Gard River, 1913km²; Vidourle River, 621km²), into hydrological meshes of 100 km².

08/09/2002; 100km²; 1h



29/10/2007; 100km²; 1h



19/10/2008; 100km²; 1h

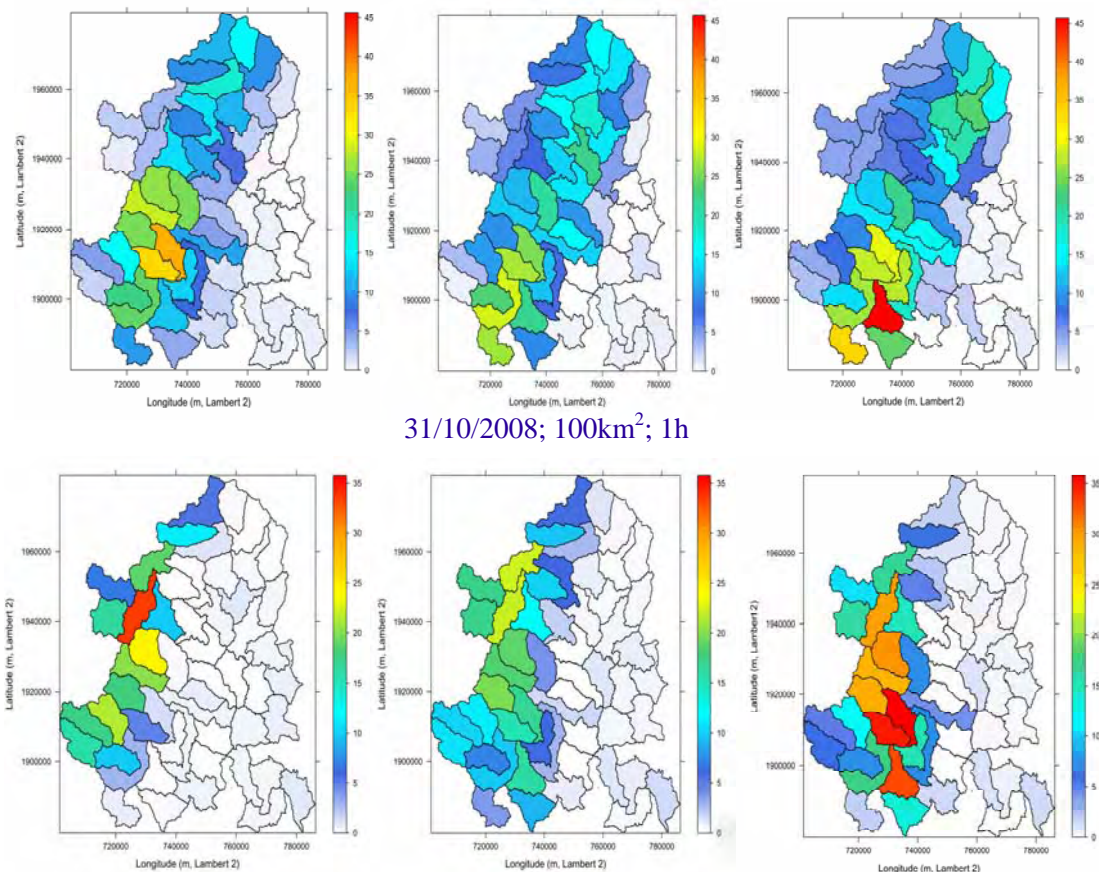


Figure 4: Examples of the evolution of rain for 3 successive hourly time steps taken during the 4 events over the main Cévennes watersheds (Ardèche River, 2500km²; Cèze River, 1054km²; Gard River, 1913km²; Vidourle River, 621km² discretized at the 100 km² scale.

In this study, we aim to analyse radar QPE uncertainties with their space – time structure by defining an empirical error model, then generate stochastically random error fields and impose them on radar measurements in order to obtain an ensemble of radar rainfall estimates. The generated radar rainfall estimates, will then, be tested with nTOPMODELS codes in order to estimate the propagation of the errors based on the simulated probabilistic discharges.

3. Radar Error model

The superposition of random and systematic errors from different sources characterizes the uncertainty of radar estimates. This work, aims to capture and study the error structure, by building up an empirical error model based on the evaluation of radar QPE accuracy with respect to an external reference. Dense rain gauge networks are generally used for this purpose although the lack on spatial representative ness.

In order to build our statistical framework, we introduce some concepts useful in the rest of this study, by noting the true unknown rainfall amount over a given area A , centered at a given location x , a given time T , centered as time i as:

$$R_{AT} = \frac{1}{A} \frac{1}{T} \iint R(u,v) dudv \quad (\text{equ.1})$$

where R denotes the true rainfall amount at a given location and time.

The radar QPE products are grided, with good spatial resolution of 1km^2 and expressed as:

$$R_{AT}^* = \frac{1}{N_A} \sum_{i=1}^{N_A} R_T^*(a_i, t) \quad (\text{equ.2})$$

where a_i represents a radar pixel, N_A is a number of pixels covering a domain A and R_T^* is the radar estimated rain amount at time t during a time interval T .

On this study, the reference rainfall was established from the available rain gauge network by using the Block Kriging technique. Reference hydrological meshes were selected based on the Kriging estimation variance (Kirstetter et al, 2010).

$$R_{AT}^{ref} = \sum_{i=1}^{N_g} \lambda_i G_T(x_i, t) \quad (\text{equ.3})$$

where $G_T(x_i, t)$ is the rain gauge amount at point x_i and time t during T and N_g is the number of rain gauges accounted for in the estimation. The coefficients $[\lambda_i, i = 1, N_g]$ are the kriging weights obtained by minimizing the estimation variance:

$$\sigma_{ref}^2 = E(R_{AT}^{ref} - R_{AT})^2 \quad (\text{equ.4})$$

under the unbiasedness condition :

$$E(R_{AT}^{ref}) = E(R_{AT}) \quad (\text{equ.5})$$

The definite advantage of this geostatistical method over concurrent interpolation technique is that the estimation variance (equ.4) provides a measure of the reference accuracy which depends on the spatial structure of the variable to be estimated and the relative configuration of the network and the domain A of interest.

The availability of such metrics, lead us to consider the residuals (rather than the ratios for instance) between the estimated and reference values as the working variable of our empirical error model.

$$\Delta_{AT}(x_i, t_k) = \Delta_{i,k} = R_{AT}^*(x_i, t_k) - R_{AT}^{ref}(x_i, t_k) \quad (\text{equ.6})$$

where k index a given integration domain of size A and i a time step of duration T

We define our empirical error model as:

$$\Delta_{i,k} = (R_k^* - R_k^{ref}) \quad (\text{equ.7})$$

where i, k index the time step and the mesh respectively.

The scatter graphs of the radar QPEs as a function of the reference rainfall and the empirical errors ($\Delta_{i,k}$) as a function of the radar QPE are presented in Figure 5 .

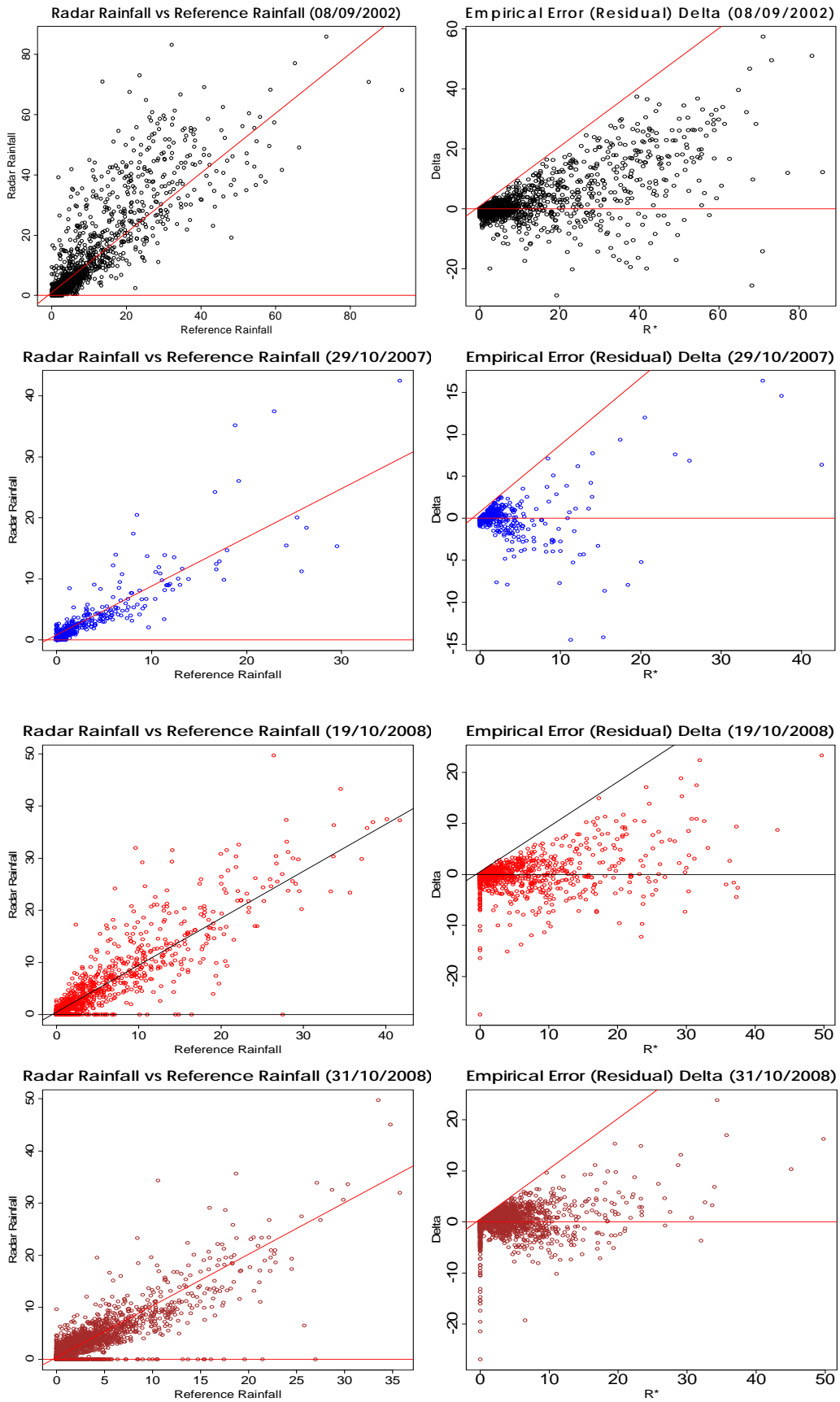


Figure 5: Scatter graphs of the evolution of the radar QPE *versus* reference rainfall (left) for the four events together with the empirical errors (residuals) as a function of radar QPE for the (100km²;1h) space-time scale (right); all the meshes and all the time steps are considered.

From Figure 5 it is clear that the variance of the error increases as radar QPE increases and that the error structure is different for each event. Note also the upper part above 1/1 line of the Delta versus radar QPE graphs appears truncated. This fact is due to the expression of $\Delta_{i,k} = (R_k^* - R_k^{ref})$: for given radar QPE value R^* , the reference rainfall can take values between 0 and infinity and so Δ varies between $-\infty$ and R^* .

In the context of this study, we therefore found important to account on the dependency of the residuals on the rain rate. For practical reasons (generation technique) we consider the dependency of Δ as a function of radar estimates. Based on that, we establish the conditional distributions of the residuals as a function of radar QPE, for a given space-time scale (100km²;1h here) using the GAMLSS framework (Stasinopoulos and Rigby, 2008). This semi – parametric model, consists of two components: a parametric probability density function (pdf) given each value of the explanatory variable and a non – parametric relationship between the pdf parameters over the domain of the explanatory variable. The conditional densities are assumed to have the same parametric form for all value of the explanatory variable (Delrieu et al, 2012). With the GAMLSS package, a wide range of two – parameters (Gaussian, t-family, p-exponential) and three – parameters (exponential-Gaussian, reverse Gumbel, gamma, log-normal etc) continuous probabilities density functions are available. Moreover, a number of non-parametric fitting techniques (cubic, penalized splines, etc) for the second component of the model are offered. Figure 6 displays the fittings obtained for three events (the fitting did not converge for the 2007 event), by grouping all the meshes (left column) and by segregating the meshes according to the range to the radar (center column: ranges greater than 60 km right column: ranges less than 60 km).

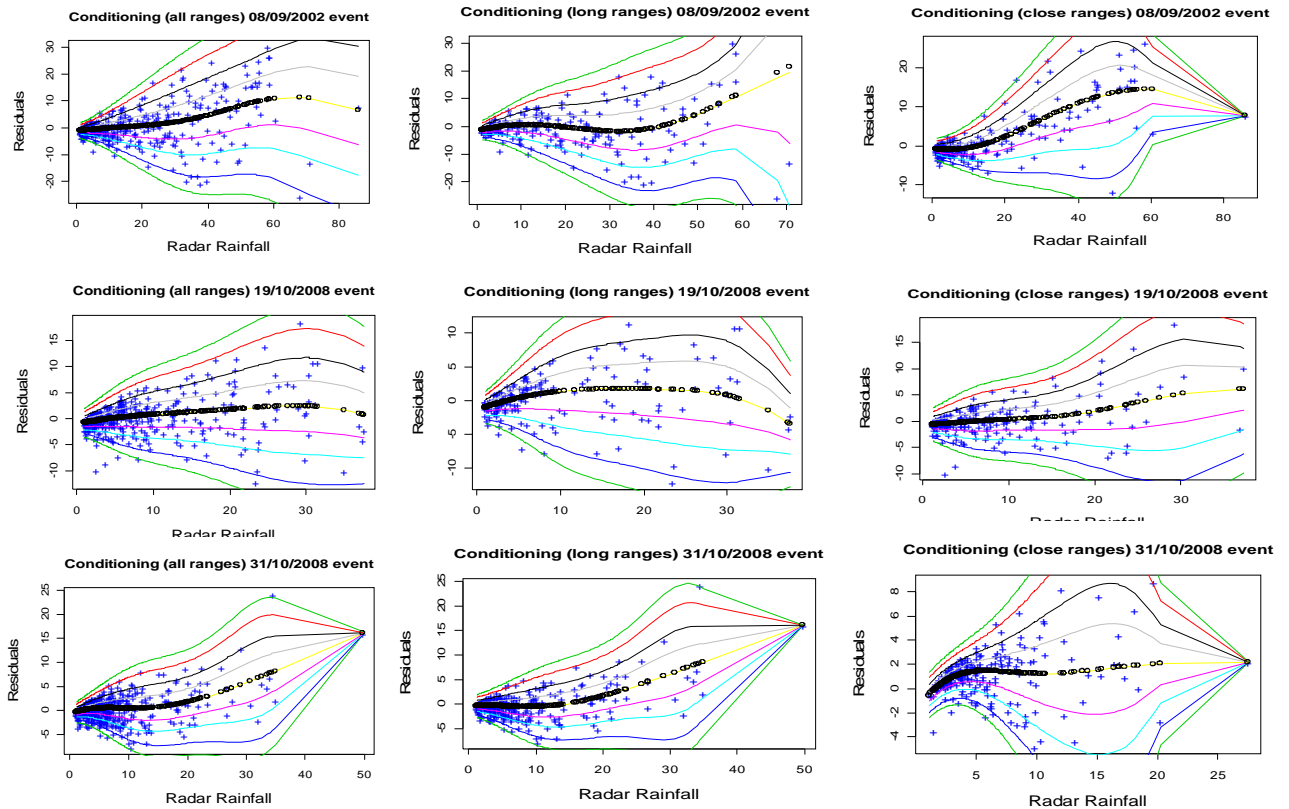


Figure 6: Scatter plot of the GAMLSS fits on the residuals $\Delta_{i,k}$ conditional on the radar QPEs for the main rain events and the (100 m²; 1 h) space-time scale. The quantiles of the Gaussian distributions are displayed together with the conditional mean (dark dotted line)

In some cases, we note there is a conditional bias, i.e. an overestimation of the residuals which tends to increase with the radar QPE, and may vary significantly according to the range from the radar. This dependency is also event dependent. We have considered various possibilities for the modeling of the residual mean. The linear regression provides us most of the time poor fits, and was varying significantly between the close and long ranges. Adapting polynomial models for the residual mean for the long and close ranges, was not very satisfactory due to the fact that those residual means are established for a series of meshes (not showed here for the sake of simplicity). According to that, we would have discontinuity, between the close and long range meshes and some problems to extrapolate the relationships. Finally, we choose two options for the mean modeling:

- Conditioning 1: use the mean model obtained from the GAMLSS analysis for all the meshes
- Conditioning 2: use of the regression between the residuals Δ and the radar estimates for each single mesh. Additionally, we forced the regression to pass by 0 in order to reduce the spread of the results for rain rates close to 0.

The code of the generator is adjusted according to these conditionings as follow:

$$\Delta_{i,n}^* = \mu(\Delta|R) + [\sigma(\Delta|R) / \sigma(\Delta)] * [\mathbf{L}y_{i,n} + \alpha_1 \Delta'_{i-1,n} + \alpha_2 \Delta'_{i-2,n}] \quad (\text{equ.22})$$

where, $\mu(\Delta_{i,k}|R)$, $\sigma(\Delta_{i,k}|R)$ are the conditional mean and standard deviation of the empirical error model, $\sigma(\Delta_{i,k})$ is the unconditional standard deviation of the empirical error model and $[\mathbf{L}y_{i,n} + \alpha_1 \Delta'_{i-1,n} + \alpha_2 \Delta'_{i-2,n}]$ is the unconditional generated perturbation field $\Delta_{i,n}$.

The evolution of the standard deviation of the conditional distribution of the error as a function of the radar QPE was found to be more or less stable between the events and the radar ranges. We have used the following expression for the first conditioning:

$$\sigma(\Delta_{i,k}|R) = 0.2R + 1 \quad (\text{equ.8})$$

For the second conditioning, the standard deviation model parameters were slightly adapted for the generated errors to match the observed ones.

Spatial and Temporal structure

In order to define the spatial structure of radar QPE uncertainties, we assume the residuals to be distributed according to usual probability distribution functions (Log-normal, Gaussian etc), so that the spatial component of the error model may be defined by the mean, the variances and the covariance of the residuals.

$$\mu_k = \frac{1}{N_T} \sum_{i=1}^{N_T} \Delta_{i,k} \quad (\text{equ.9})$$

$$C_{kk} = \frac{1}{N_T} \sum_{i=1}^{N_T} (\Delta_{i,k} - \mu_k)^2 \quad (\text{equ.10})$$

$$C_{k,m} = \frac{1}{N_i} \sum_{i=1}^{N_T} (\Delta_{i,k} - \mu_k)(\Delta_{i,m} - \mu_m) \quad (\text{equ.11})$$

where k index the mesh and N_i the number of time steps.

We estimate the mean and the variance/covariance matrix between all meshes of the discretized watersheds for the four events, so as to have an approximation of the spatial structure of the residuals and to compute the uncertainties in our empirical error model. μ is a vector that contains the mean value for each mesh k and for all time step i , while the $C_{k,m}$ is a matrix with values of the covariance between k,m meshes in its entries.

$$\mu = (m_{u1}, m_{uk}, \dots, m_{uNm}) \quad (\text{equ.12})$$

where Nm is the number of meshes

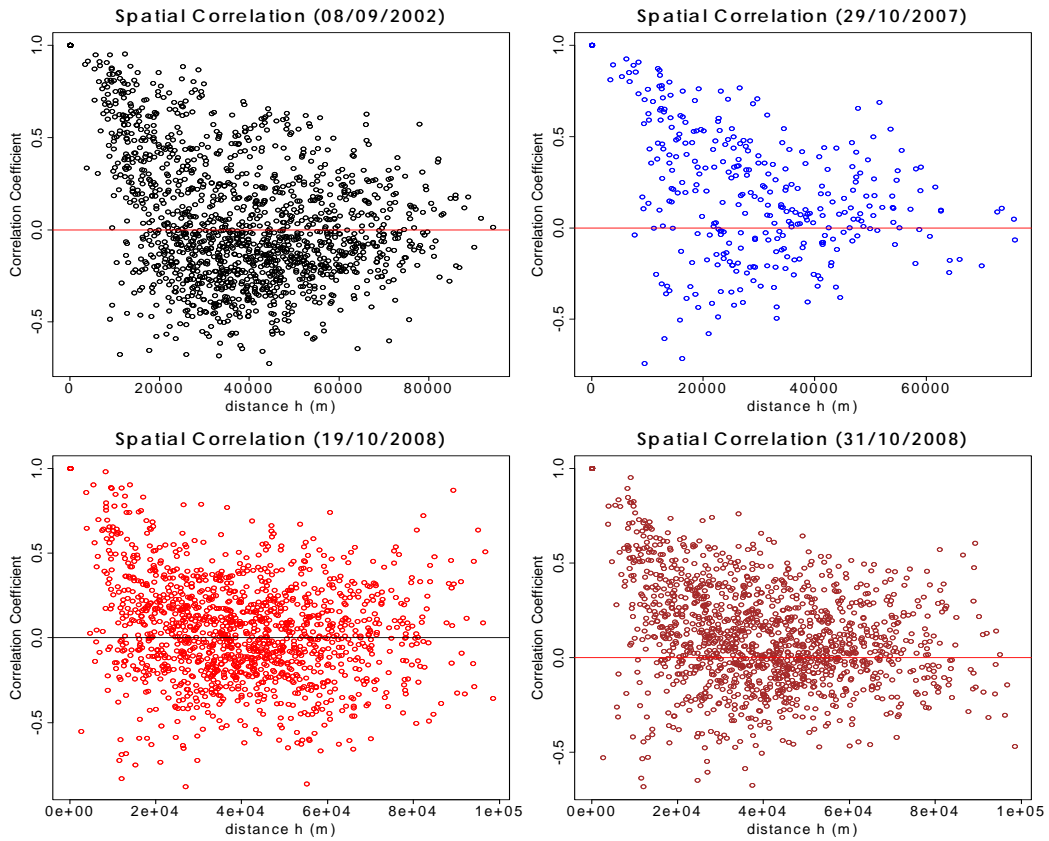


Figure 7: Spatial structure of the empirical error model $\Delta_{i,k}$, as a function of the distance between the meshes.

Figure 7 displays the correlation coefficients as a function of the distance between the center of the meshes for the various events. For a distance of 20 km, the correlation lies between 0.5 and 0.9 indicating that the errors are significantly correlated in space. For distances of 40 to 60 km the correlation drops to values around zero and below.

For the temporal structure, the autocorrelation function in order 1 and 2 were calculated locally for each mesh using (13) and the variability of the temporal error structure for all the meshes, is presented in Figure 7.

$$C_{k,j} = \frac{1}{N_T} \sum_{i=1}^{N_T} (\Delta_{i,k} - \mu_k)(\Delta_{(i+j),k} - \mu_k) \quad (\text{equ.13})$$

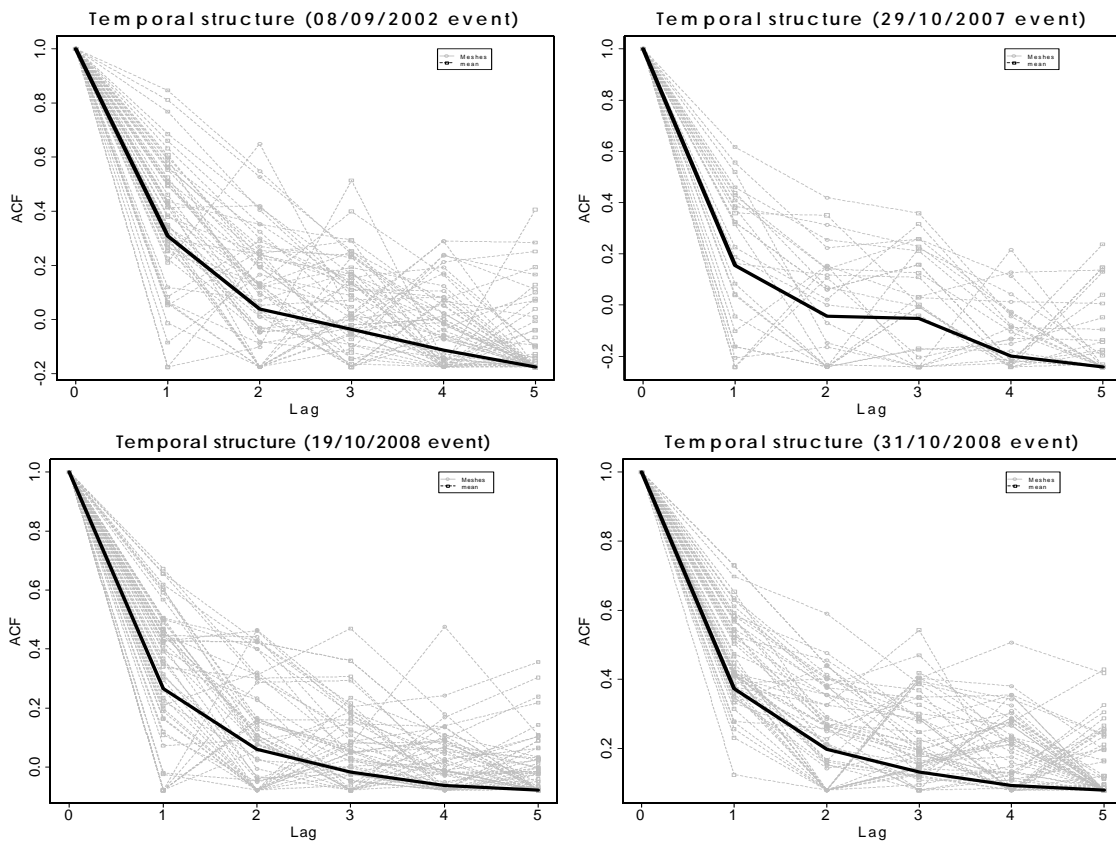


Figure 8: Temporal structure of the empirical $\Delta_{i,k}$, for the four main rain events. The autocorrelation function for lag time 1 to 6 is presented with the dotted line and the mean value with the black solid line for each of the events

From Figure 8, it can be obtained, that there are some significant correlation of order 1 for the majority of the meshes and for all of the four events. The temporal correlation at lag 1 (1 hour) is comprised between 0.2 and 0.6. However, for the 2002 event, there are two meshes, (mesh 37, mesh 38), with high correlation of order one ($r_1 = 0.78$, mesh2=0.8 respectively). For lag 2, the mean temporal correlation is about 0.2, indicating the rather weak temporal correlation of the errors for the considered space-time scale.

4. Ensemble Generation

The main idea is to generate random Gaussian additive error fields, accounting for the empirical space-time structure identified in section 3, and then add them to the original radar QPE. Thus we would get a set of probabilistic radar QPE (PQPE) to be used as input to hydrological model to assess model uncertainties. The algorithms that were implemented in this study were proposed in a paper by Germann et al (2009). We have extended this approach by accounting for the dependency of the errors on the radar QPE evidenced in Section 3.

$$\mathbf{F}_{i,n} = \mathbf{R}_i - \Delta_{i,n} \quad (\text{equ.14})$$

where $\mathbf{F}_{i,n}$ is vector of the resulting precipitation values for the N meshes for a given time step i and for an ensemble member n ; \mathbf{R}_i is the vector of the original radar rainfall QPEs at time i while $\Delta_{i,n}$ is the vector of the Gaussian perturbations for a given time step i , and ensemble member n .

The first term of (equ.14) presents the probabilistic precipitation components while the \mathbf{R}_i is the deterministic radar field and the $\Delta_{i,n}$ is the stochastic component. For a given domain A , usually a watershed, the probabilistic precipitation field, give us N realizations of rainfall for k number of meshes and time step i , while the stochastic component $\Delta_{i,n}$ is consistent with the space – time structure of radar uncertainties. The N realizations can be used as input to hydrologic model, yielding a distribution of response values, the spread of which presents the propagation of the radar precipitation error.

The core of the ensemble generator relies on the establishment of the perturbation field. In order to have the space – time correlated perturbation field $\Delta_{i,n}$ it is important to introduce a technique to produce these Gaussian fields. The most versatile technique is the LU decomposition on the symmetric positive definitive covariance matrix of the residuals (Germann et al 2009):

$$\mathbf{C} = \mathbf{L}\mathbf{L}^T \quad (\text{equ.15})$$

We obtain the perturbed vector $\Delta_{i,n}$ by multiply a random Gaussian vector $\mathbf{y}_{i,n}$ with the “square root” of the covariance matrix of the residuals. The decomposition obtained by the LU algorithm expresses the covariance matrix as the product of a lower and an upper triangular matrix. Thus, the resulting perturbation fields $\Delta_{i,n}$ are spatial correlated Gaussian with pre-defined covariances. The LU decomposition offers full flexibility regarding space – time dependence of errors (Goovaerts, 1997).

$$\Delta_{i,n} = \mathbf{L}\mathbf{y}_{i,n} \quad (\text{equ.16})$$

where i,n are the time step and the ensemble member respectively.

As a next step, we use the $AR(2)$ filtering for each one of the discretized meshes of the generated random errors $\Delta_{i,n}$ so that to impose the desired temporal structure. Utilize the

$AR(2)$ model, we calculate the perturbation field for a time step i and mesh k , by combining $\mathbf{L}y_{i,n}$ with the $AR(2)$ filtered perturbation fields of the previous two time steps $i-1$ and $i-2$. Two parameters a_1, a_2 were used, obtained by the Yule – Walker equations (Priestley, 1981) together with the square root of the $AR(2)$ variance rescaling factor U . It is important to utilize the rescaling factor U , since with the $AR(2)$ model, the variance changes by a linear factor, depending on the model parameters a_1, a_2 . The mean value of its mesh is added in the end of this procedure in order to correct the generated $\Delta_{i,n}$ in terms of bias.

$$\Delta'_{i,n} = \mathbf{L}y_{i,n} + a_1\Delta'_{i-1,n} + a_2\Delta'_{i-2,n} \quad (\text{equ.17})$$

$$\Delta_{i,n} = \mu + U\Delta'_{i,n} \quad (\text{equ.18})$$

$$a_1 = \frac{r_2 - 1}{1 - r_1^2} \quad (\text{equ.19})$$

$$a_2 = \frac{r_1^2 - r_2}{1 - r_1^2} \quad (\text{equ.20})$$

$$U = \left[\frac{1 + a_2}{(1 - a_2)(1 - a_1 + a_2)(1 + a_1 + a_2)} \right]^{-0.5} \quad (\text{equ.21})$$

In order to account for the dependency show in Section 3 and since the relationship described the sigma parameter is more or less constant, we use a linear relationship for the conditional standard deviation ($\sigma(\Delta_{i,k}|R) = 0.2R + 1$) and we considered two possibilities for accounting for the conditional bias. The code of the generator was adjusted according to these two conditionings.

1st Conditioning

The first conditioning is implemented to (100km²; 1h) space- time scale hydrological meshes and we utilize the conditional mean and the approximate conditional sigma parameter (equ.8) derived from all the meshes with the GAMLSS model. For the sake of simplicity we note the conditional, generated perturbation fields as $\Delta_{i,n}^*$.

It was estimated that the variability using the 1st Conditioning was mostly affected by the evolution of the $\sigma(\Delta_{i,k}|R)$ parameter rather than the conditional mean. Therefore, for the 2008 events, we adapt the conditional sigma so that to be closer to the empirical model $\Delta_{i,n}$, while for the 29/10/2007 event, this 1st Conditioning was not implemented because the GAMLSS fit did not converge. Generally, it was estimated that using the global mean, could not account for producing the variability that we have in the observed $\Delta_{i,k}$ (Figures 9;10;11;12).

2nd Conditioning

In the 2nd conditioning, we use the conditional mean specific to each mesh with the conditional sigma parameter obtained from the GAMLSS model. The conditional mean is estimated by fitting a linear regression to the errors versus the radar QPEs for each single mesh. We found useful to force the regression offset to 0 so as to reduce the spread of the values around zero and to be closer to the empirical model. It was found necessary to adapt the parameters of conditional standard deviation for the 19/10/2008 and 31/10/2008 events with the use of the $\sigma(\Delta_{i,n}|R)$ model fitted from the GAMLSS approach. For the 29/10/2007 event we used $\sigma(\Delta_{i,n}|R) = 0.2R$ and the study was focused on the Vidourle and Gardons watersheds.

The results for the 1st and the 2nd conditionings as well as for the unconditioned cases for all the events are presented in presented in Figures 9-12. Considering the 2nd conditioning, we were able to generate conditioned error fields $\Delta_{i,n}$, based on more realistic results compared to the empirical error model, by adapting the conditioned mean $\mu(\Delta_{i,k}|R)$ and the sigma parameter $\sigma(\Delta_{i,k}|R)$. For the 08/09/2002 events the utilize of these parameters helped to produce the variability that we observe in the empirical error model even though there is an increase of the spread of the negative values. For the 29/10/2007 the variability from the empirical error model cannot be generated totally even if we adapt the conditional sigma parameter while for the 19/10/2008 and 31/10/2008 events there were some unrealistic values of radar errors above the (1,1) line.

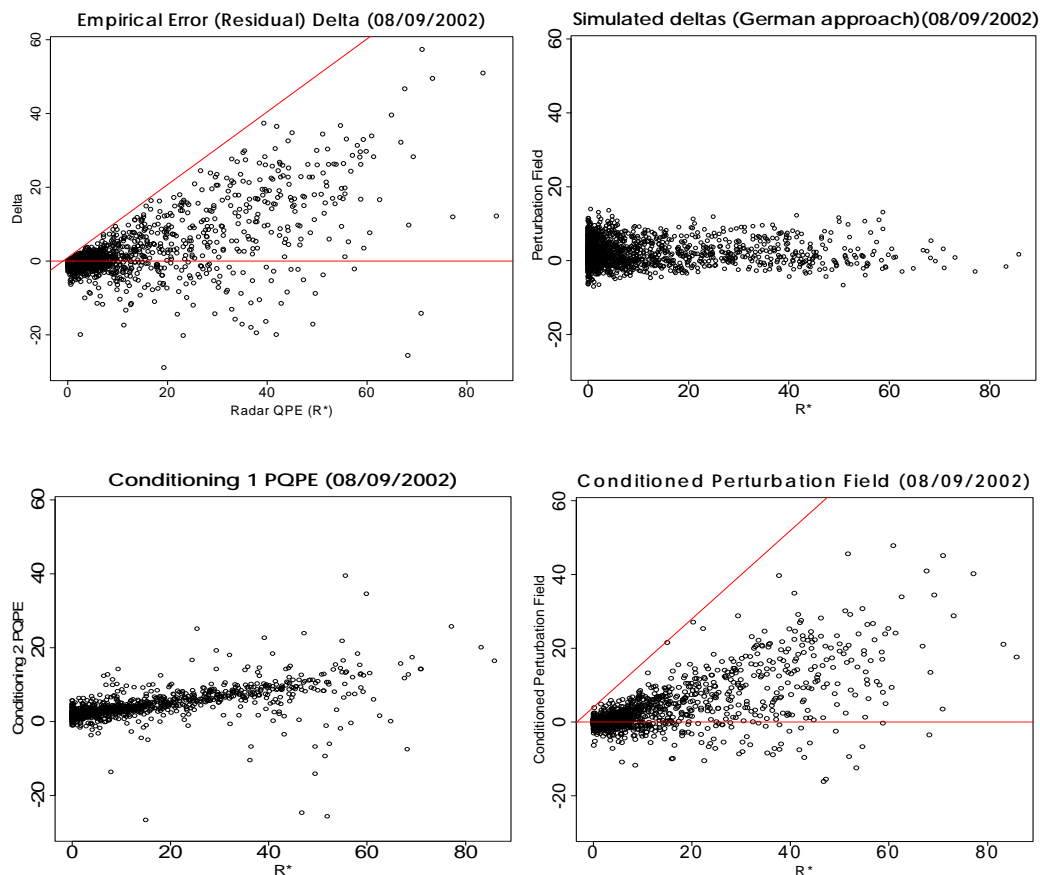


Figure 9: Scatter plots of observed and simulated errors for the 08/09/2002 event as a function of the radar QPEs. The errors derived from the observations (up, left), the unconditioned generator (up, right) and the conditionings 1 (bottom, left) and 2 (bottom, right) are displayed.

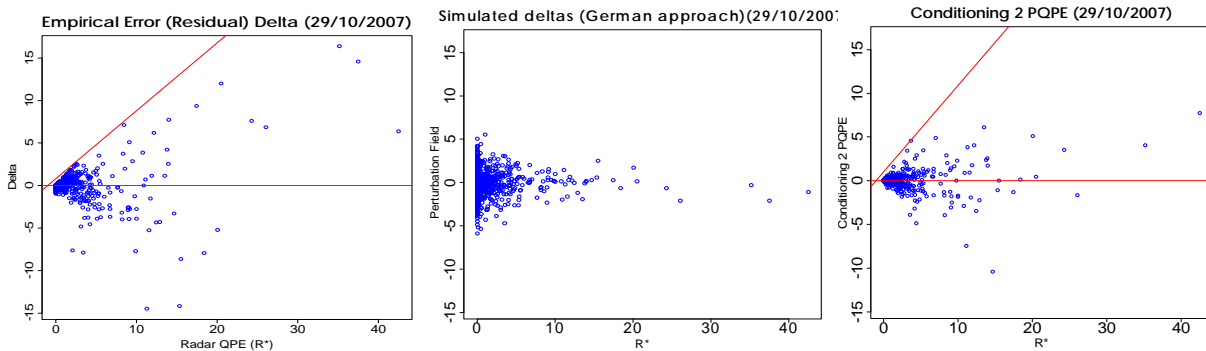


Figure 10: Scatter plots of observed and simulated errors for the 29/10/2007 event as a function of the radar QPEs. The errors derived from the observations (left), the unconditioned generator (right) and the conditioning 2 (right) are displayed.

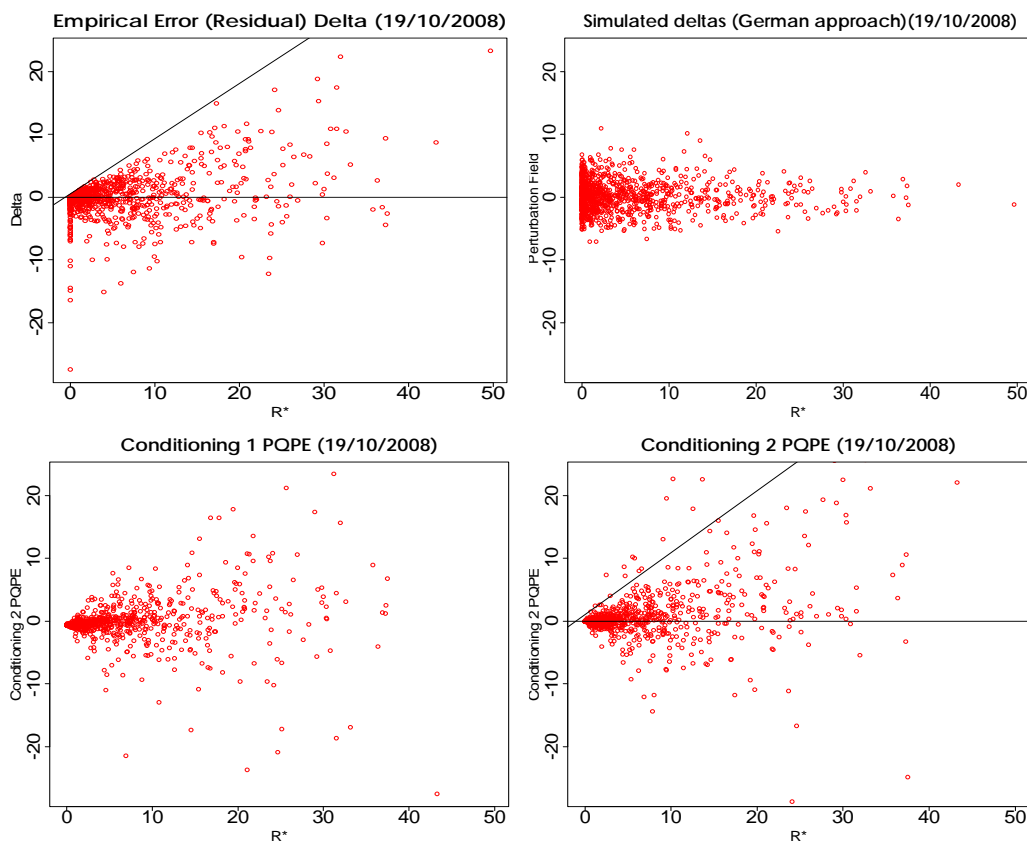


Figure 11: Scatter plots of observed and simulated errors for the 19/10/2008 event as a function of the radar QPEs. The errors derived from the observations (up, left), the unconditioned generator (up, right) and the conditionings 1 (bottom, left) and 2 (bottom, right) are displayed.

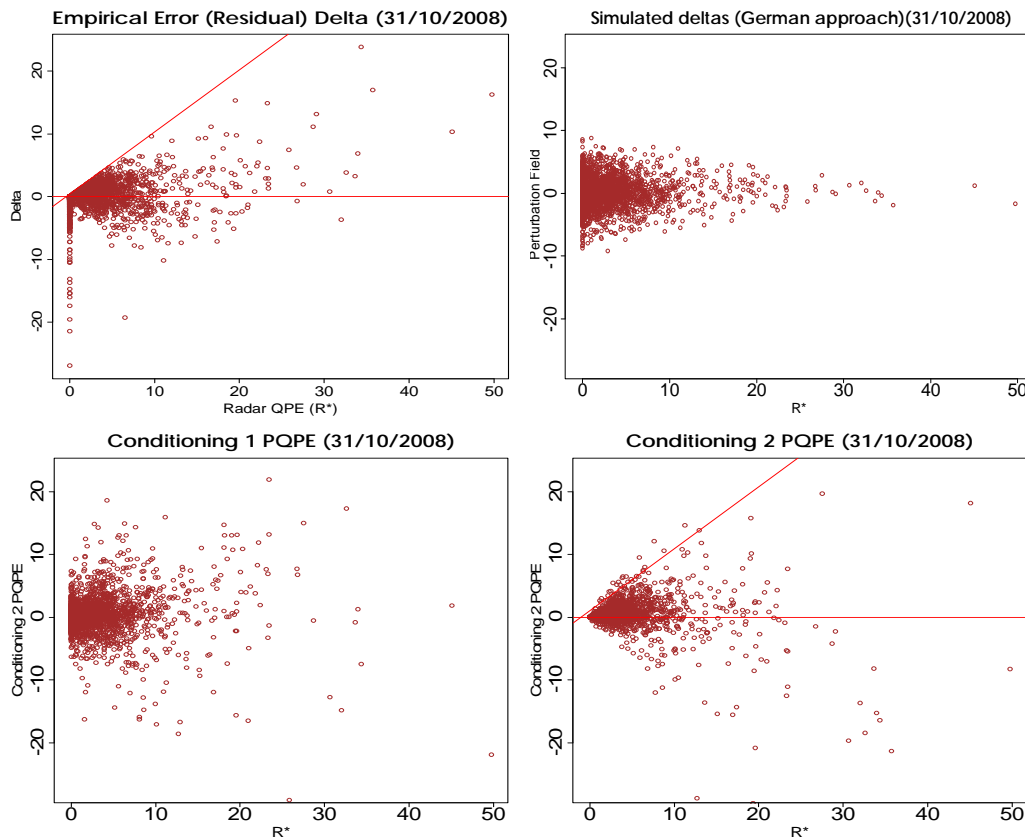
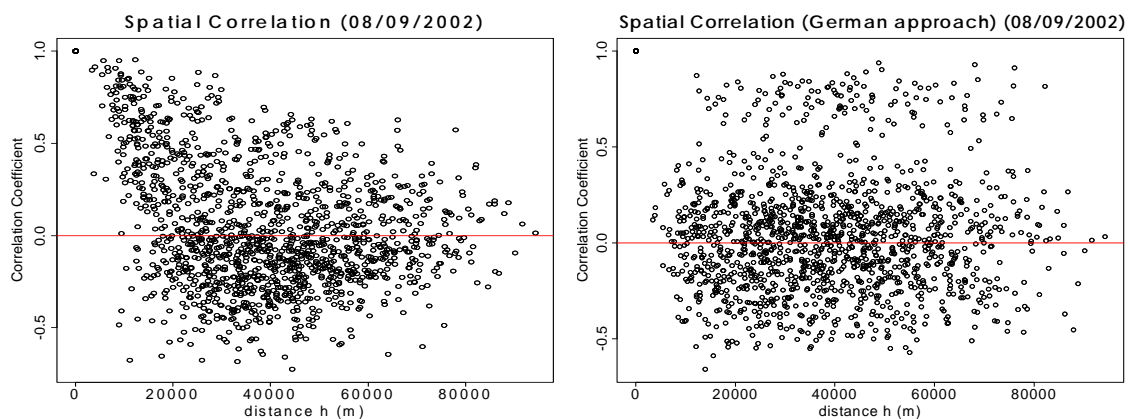


Figure 12: Scatter plots of observed and simulated errors for the 31/10/2008 event as a function of the radar QPEs. The errors derived from the observations (up, left), the unconditioned generator (up, right) and the conditionings 1 (bottom, left) and 2 (bottom, right) are displayed.

4.1. Impact of the conditionings on the temporal and spatial structure of the simulated errors

In order to be more accurate for the results, we obtained the influence of the conditionings on the space – time structure of the simulated errors versus the observed errors. The results of the temporal and spatial structure obtained for the 08/09/2002 event are showed in Figure 13; 14.



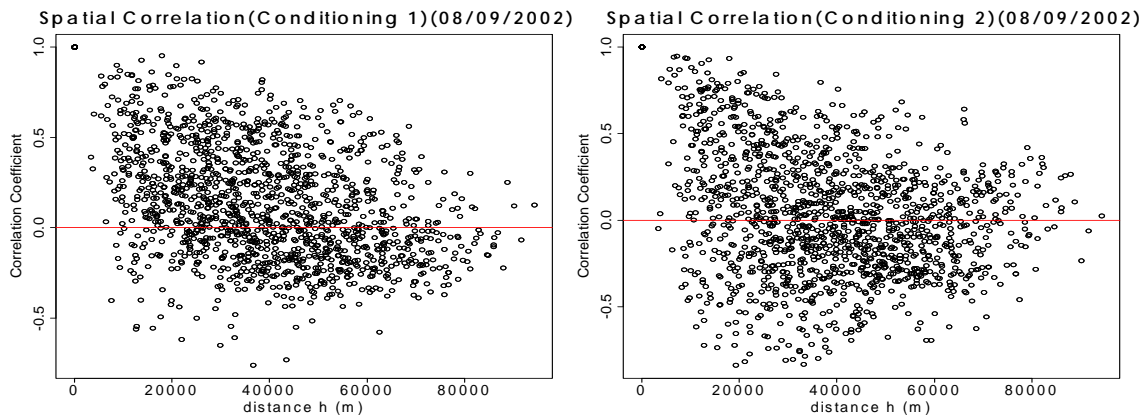


Figure 13: Spatial structure of the simulated errors, as a function of the distance between the meshes; the spatial structure of the empirical error model is presented in the upper left graph while the spatial variability of the unconditioned, 1st conditioning, 2nd conditioning are showed in the upper right, down left and down right graphs respectively

From Figure 13 compared to Figure 7 it can be estimated, that still for 20km there is a spatial correlation of the errors between 0.5 – 0.9 both for the 1st and the 2nd conditioning, while for the unconditioned situation the spatial structure is altered on an important degree.

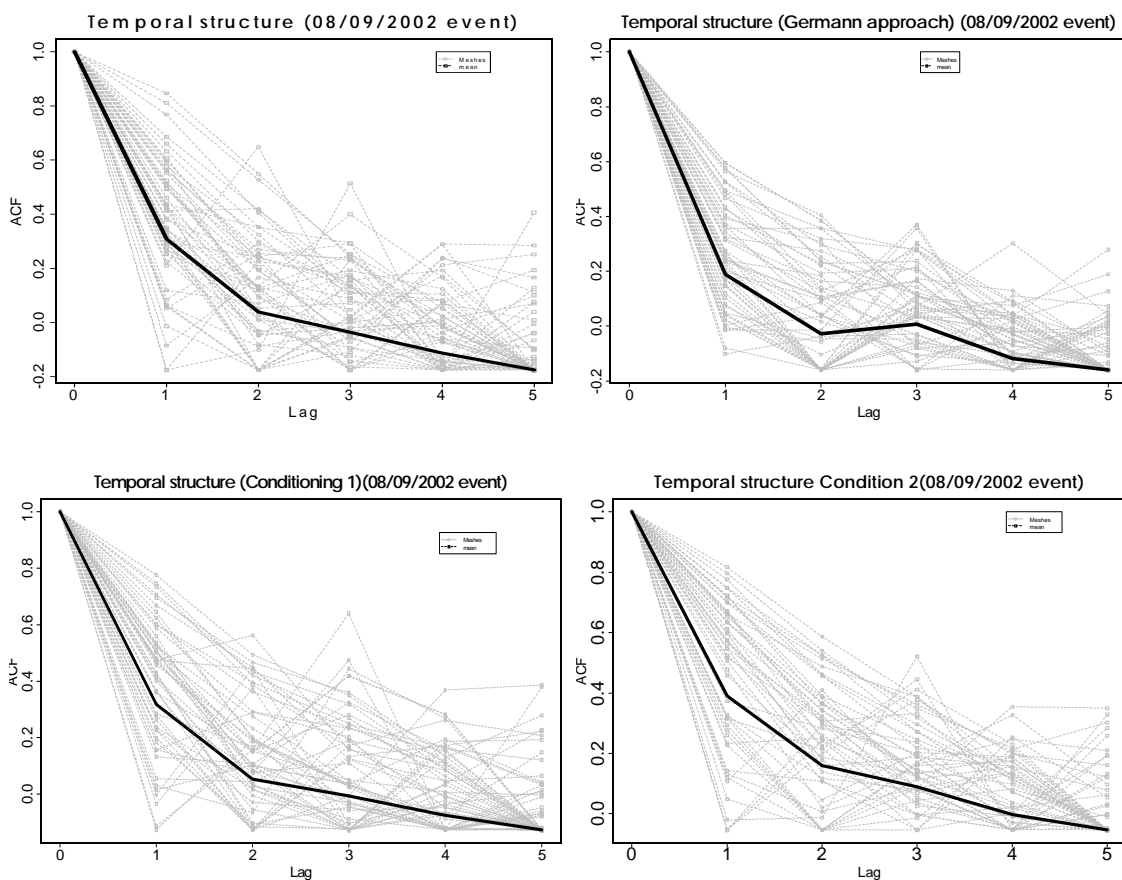


Figure 14: Temporal structure of the simulated errors, for the four main rain events. The autocorrelation function for lag time 1 to 6 is presented with the dotted line and the mean value with the black solid line; the temporal structure of the empirical error model is presented in the upper left graph while the temporal variability of the unconditioned, 1st conditioning, 2nd conditioning are showed in the upper right, down left and down right graphs respectively

From Figure 14 compared to Figure 8 , it can be obtained that there is a significant temporal correlation at 1h time step, while we can estimate that we do not change the temporal structure of the errors so much (unconditioned situation.). The temporal correlation ,drops to 0.2 in the 2nd time step for the majority of the meshes .

Examples of hyetographs

The generated Deltas for the four main rain events (08/09/202, 29/10/2007, 19/10/2008, 31/10/2008) and for 100km² meshes of each of the watersheds (Ardèche, Vidourle, Céze and Gardons) were simulated 50 times and the error was subtracted to the radar QPE (due to the definition of the errors (equ.7)), in order to obtain the probabilistic QPEs. We present some hyetographs obtained for the 08/09/2002 event: the 50 simulations with the unconditioned situation, 1st and the 2nd conditionings compared to the radar estimates and reference time series are presented in Figures 13 and 14 for two meshes which exhibit contrasted behaviour.

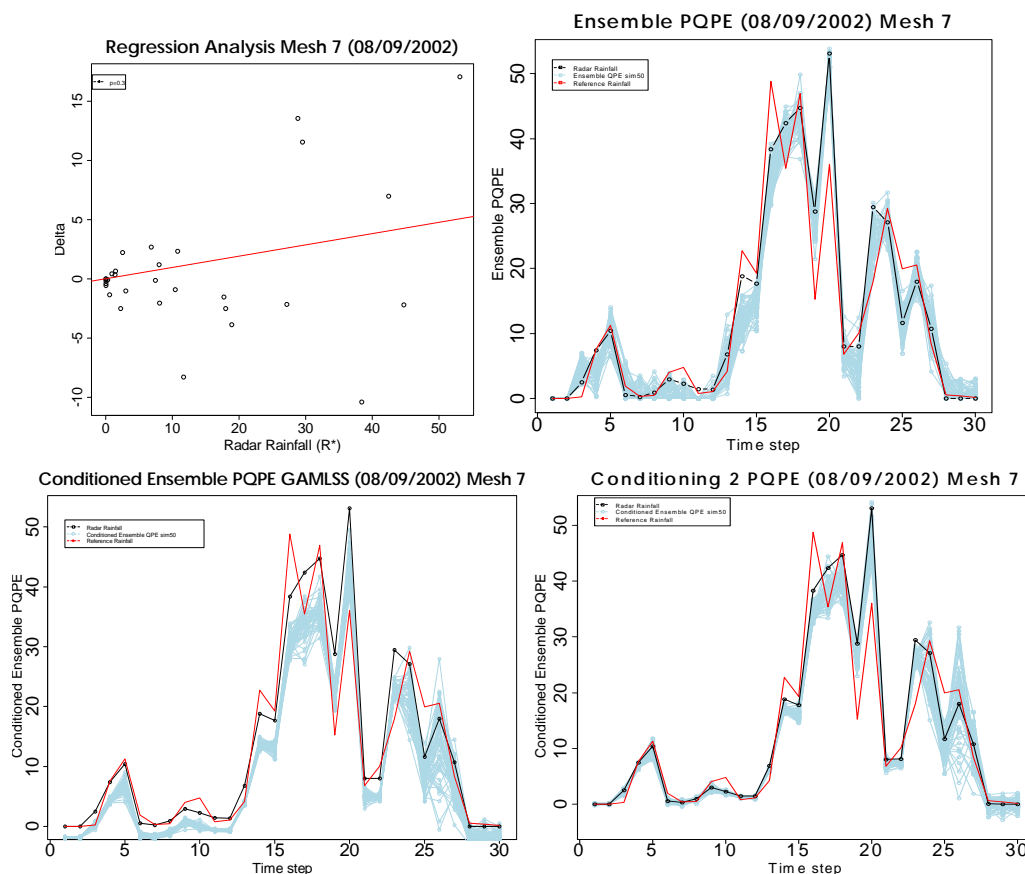


Figure 15: Probabilistic QPE (PQPE) with the unconditioned situation (top right), 1st (bottom left) and the 2nd (bottom right) conditioning for given meshes for the 08/09/2002 event; the radar QPE, the reference rainfall and the 50 simulations are displayed on the graphs with the black, red, light blue lines respectively; the regression analysis of the errors as a function of the radar QPE for the given mesh ($\rho=0.3$) is also displayed (top left)

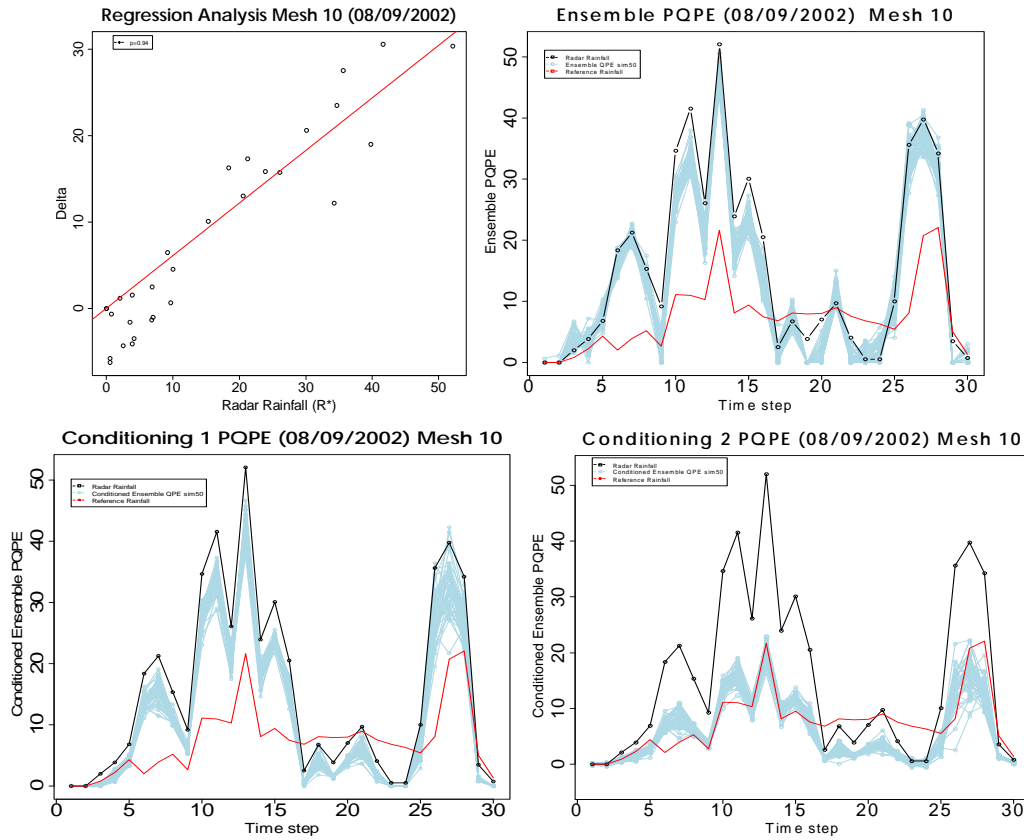


Figure 16: Probabilistic QPE (PQPE) with the unconditioned situation (top right), 1st (bottom left) and the 2nd (bottom right) conditioning for given meshes for the 08/09/2002 event; the radar QPE, the reference rainfall and the 50 simulations are displayed on the graphs with the black, red, light blue lines respectively; the regression analysis of the errors as a function of the radar QPE for the given mesh ($\rho=0.94$) is also displayed (top left)

Table I: Statistical parameters for the validity of the results; the mean; correlation; standard deviation; Kriging estimation variance are displayed

	Mesh ₇	Mesh ₁₀
M^{ref}	12.5	7.47
M^*	13.14	15.50
M^* / M^{ref}	1.05	2.07
$Cor(R_k^{ref}, R_k^*)$	0.93	0.7
$\sigma_{kriging}^2$	0.08	0.5
M^{Delta}	0.6	8.03
sd^{Delta}	5.53	11.3
$M_{conditional1}^{regression}$	$\mu(\Delta_{i,k} R_k^*) = 0.16R + 1.78$	
$M_{conditional2}^{regression}$	$\mu(\Delta_{i,k} R_k^*) = 0.09R$	$\mu(\Delta_{i,k} R_k^*) = 0.6R$

In Figure 15, the consistency of the radar QPE with respect to the reference rainfall is rather good with a bias of $M^* / M^{ref} = 1.05$ and a correlation coefficient of 0.93. Note that the quality of the reference is good with a normalised Kriging estimation variance of 0.08. The unconditioned generation leads to realistic hyetographs with quite a uniform spread of the ensemble whatever the radar QPE. Conditioning 1, based on the correction of the conditional bias calculated over all the meshes, tends to under-estimate the PQPE compared to both the reference and the radar QPE; one may note that, as expected, the variability of the PQPE depends now on the radar QPE. Conditioning 2 utilizes the regression analysis of the errors as a function of the radar QPE: in that case the correlation is poor and therefore the conditional mean dependency on the radar QPE is low. The mean values of the unconditioned *Deltas* of the meshes₇, mesh₁₀, are estimated to be of order 0.6, 8.03 while the standard deviation for the given meshes is equal to 5.53, 11.3 respectively. Concerning the conditional statistical parameters, are estimated to be for the meshes₇, mesh₁₀: conditional mean equal to 3.98 and 5.36 and the standard deviation of order 6.98 and 7.48 respectively. We note that the bias correction is lower than for conditioning 1.

In Figure 16, the consistency of the radar QPE with respect to the reference rainfall is much lower compared to the previous case ($M^* / M^{ref} = 2.07$; $Cor(R_k^{ref}, R_k^*) = 0.7$). The radar QPE strongly overestimates the rainfall compared with the reference time series. Note that the quality of the reference is not good with a normalised Kriging estimation variance of 0.5. As in Fig. 15, the unconditioned generation leads to realistic hyetographs with quite a uniform spread of the ensemble whatever the radar QPE. Conditioning 1, based on the correction of the conditional bias calculated over all the meshes, slightly reduced the bias of the PQPE with respect to the reference. Conditioning 2 utilizes the regression analysis of the errors as a function of the radar QPE: in that case the correlation is good and therefore the conditional mean dependency on the radar QPE is high. We note that, due to the accounting of the local conditional bias, the PQPE tend to present a very good agreement toward the reference hyetograph. A desirable evolution of the method would be to account for the quality of the reference rainfall to decide if such a bias correction is desirable or not. In the present case, due to the high Kriging estimation variance, it could be suggested to use Conditioning 1 for this specific mesh.

5. Hydrological modeling

The topographic based hydrological model, Topmodel, presented by Beven & Kirby (1979), conceptualizes the soil water storage as a sequence of storages with different properties. This hydrologic model, predicts the catchment's responses following one, or a series of rainfall events (Chairat et al, 1993). It constitutes one of the first models representing the lateral subsurface flow in the first meters of soil which leads to the generation of runoff on saturated areas of the catchments. Some points of a watershed do not have hydrodynamic behaviour (hydraulic transmissivity, hydraulic gradient etc.), allowed them to evacuate from the upstream the amount of water that reaches. These points become superficial saturated, since the received water runs mostly to the water system. Such hydrological processes have been proved to dominate in the genesis of flash floods in the region of Cèvennes - Vivairais (Lardet and Obléd, 1994, Saulnier and Datin, 2004).

The version of Topmodel that was used was developed at LTHE (Saulnier et al. 1997; Saulnier and Datin, 2004). This version, called n-Topmodel is a distributed version where the watershed of interest is divided into hydrological meshes of about the same size (100 km² herein). For each mesh, four parameters are to be specified:

- The surface hydraulic conductivity (K; m.s-1)
- The exponential decay of conductivity with the depth (m (m)).
- The water content of the layer of topsoil at the beginning of the event (SRMax (m)).
- The rate of evapotranspiration losses (Inter (m.s-1)).

The spatial discretization of the basin is achieved through a mesh which, in a given region, to derive Digital Terrain Model (DTM) surfaces of irregularly shaped and size selected by the user (see Figure 2). The jagged edges of these surfaces meet and define the topography and hydrology of the mesh to the contours of zero flows. Modeling n-TOPMODEL comes from a spatialization of TOPMODEL on this mesh.

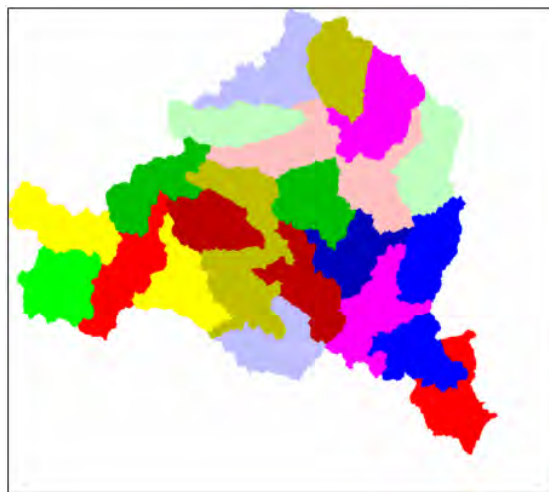


Figure 17: Example of the discretization of the Ardèche watershed provided in to hydrological meshes 100km²

Unfortunately, time was missing during the project to implement and finalize the hydrological modelling with the available PQPEs.

6. Conclusions

This work, presents a probabilistic approach to represent the uncertainty in radar estimates by providing a statistical framework for producing an ensemble of precipitation fields. The methodology addressed so as to provide a preliminary version of an error model for radar QPE in the context of the Cévennes–Vivairais Mediterranean Hydro-meteorological Observatory window (CVMHO) using radar and rain gauge datasets. This error model was designed with respect to the reference rainfall data from available rain gauge network by using the Block Kriging technique, while reference hydrological meshes were selected based on the Kriging estimation variance. The empirical errors, designed for four events, where it was estimated that the different error structure for each of the events and it was clear the increase of the variance of the errors.

On the context for dependency of the errors as a function of radar QPE, the conditional distribution of the errors obtained for all the 100km²; 1h hydrological meshes and according to

the range from the radar showed that, in some cases there is a conditional bias, meaning, an overestimation of the errors which tends to increase with the radar estimates. This dependency varies significantly between close and long ranges, while is also event dependent. For modeling the conditional mean of the error, several approaches was taken into account by using linear or polynomial models which led to no satisfactory results. Thus, regression analysis of the errors versus the radar estimates was conducted. In order to account on the conditional bias, two possibilities of conditioning were used.

The results confirmed that radar rainfall estimates have a complex error structure. Radar errors showed a temporal and a spatial structure which has to be taken into account for rain field simulation. From the generation of the PQPE, it was obtained that, when there is a good agreement between the radar estimates and reference rainfall but poor correlation between the radar estimates and the errors, the 1st conditioning tends to improve in terms of bias but with a significant underestimation, while in the 2nd conditioning, the dependency of the conditional mean on the radar estimates is low. However, with good correlation between the errors and the radar estimates but without accounting of the accuracy of the reference, the 1st conditioning reduces in terms of bias, and in the 2nd conditioning there is a good agreement of the spread of the ensemble around the radar estimates.

Considering the radar data processing and parameterization with the dependency of the error model on climatological context, some factors may have significant influence on the empirical results. These, include residual beam blockage effects, uncertainty in the Z-R relationship caused by variability of the drop-size distribution and erroneous rain gauge measurements remaining after quality control.

To sum up, concerning the results that were obtained through the generation of the QPE ensemble we are now confident in the calculations of the code. It would be desirable to account for the accuracy of the reference rainfall in conditioning 2. The study of the propagation of the precipitation error with the n-Topmodel codes remains to be undertaken, as well as a sensitivity study on the space-time scales considered..

References

- Austin PM. 1987. Relation between measured radar reflectivity and surface rainfall. *Mon. Weather Rev.* 115: 1053–1070.
- Bellon A, Lee G, Kilambi A, Zawadzki I. 2007. Real-time comparisons of VPR-corrected daily rainfall estimates with a gauge mesonet. *J. Appl. Meteorol.* **46**: 726–741.
- Berenguer M, Corral C, S´anchez-Diezma R, Sempere-Torres D. 2005. Hydrological validation of a radar-based nowcasting technique. *J. Hydrometeorol.* **6**: 532–549.
- Berenguer M, Sempere-Torres D, S´anchez-Diezma R, Pegram G, Zawadzki I, Seed A. 2006.. ‘Modelization of the uncertainty associated with radar-based nowcasting techniques. Impact on flow simulation’. Pp 575–578 in Proc. 4th European Conf. on Radar in Meteorology and Hydrology, 18–22 September 2006, Barcelona, Spain.
- Berenguer M., Zawadzki I., 2008. A study of the error covariance matrix of radar rainfall estimates in stratiform rain. *Weather Forecast* 23 (6), 1085-1101.
- Beven, K.J. & Kirby, M.J. (1979). A Physically Based, Variable Contributing Area Model of Basin Hydrology, *Hydrol. Sci. J.* **24**(1), 43-69
- Bonnifait, L., et al. (2009), Hydrologic and hydraulic distributed modelling with radar rainfall input: Reconstruction of the 8-9 September 2002 catastrophic flood event in the Gard region, France., *Advances in Water Resources*, 32, 1077-1089.
- Borga, M. (2002). “Accuracy of radar rainfall estimates for stream flow simulation.” *J. Hydrol.*, 267, 26–39.

- Bouilloud, L., Delrieu, G., Boudevillain, B., Kirstetter, P.E., 2010. Radar rainfall estimation in the context of post-event analysis of flash-flood events. *J. Hydrol.* 394 (1–2), 17–27.
- Bowler NE, Pierce CE, Seed AW. 2006. STEPS: A probabilistic precipitation forecasting scheme which merges an extrapolation nowcast with downscaled NWP. *Q. J. R. Meteorol. Soc.* **132**: 2127–2155.
- Carpenter T.M., Georgakakos K.P., 2003. Distributed model flow sensitivity to uncertainty in radar rainfall input, *Weather Radar Information and Distributed Hydrological Modelling* {Proceedings of symposium IIS03 held during IUGG2003 at Sapporo. July 2003}. IAHS Publ. no. 282.
- Chairat S., Delleur J.W.. Intergrating a physical based hydrological model with Grass, HydroGIS 93:IAHS, Publ. No 211,1993
- Creutin, J.D., Borga, M., 2003. Radar hydrology modifies the monitoring of flash flood hazard. *Hydrol. Processes* 17 (7), 1453–1456.
- Delrieu, G., Boudevillain, B., Nicol, J., Chapon, B., Kirstetter, P.E., Andrieu, H., Faure, D., 2009. Bollène 2002 experiment: radar rainfall estimation in the Cévennes– Vivarais region, France. *J. Appl. Meteorol. Climatol.* 48, 1422–1447.
- Delrieu, G., Bonnifait, L., Kirstetter, P., Boudevillain, B., 2012. Dependence of radar quantitative precipitation estimation error on the rain intensity in the Cévennes region, France. *Hydrological Sciences* (under review).
- Germann U, Joss J. 2002. Mesobeta profiles to extrapolate radar precipitation measurements above the Alps to the ground level. *J. Appl. Meteorol.* **41**: 542–557.
- Germann U, Berenguer M, Sempere-Torres D, Salvad`e G. 2006a. ‘Ensemble radar precipitation estimation – A new topic on the radar horizon’. Pp 559–562 in Proc. 4th European Conf. on Radar in Meteorology and Hydrology, 18–22 September 2006, Barcelona, Spain.
- German U., Berenguer M., Sempere-Torres D., Massimiliano Z. 2009. *Ensemble radar precipitation estimation for hydrology in a mountainous region (REAL)*, Quarterly Journal of the Royal Meteorological Society, *Q. J. R. Meteorol. Soc.* **135**: 445–456 (2009)
- Jordan, P.W., Seed, A., Weinmann, P.E., 2003. A stochastic model of radar measurement errors in rainfall accumulations at catchment scale. *J. Hydrometeorol.* 4 (5), 841–855.
- Joss J, Lee R. 1995. The application of radar-gauge comparisons to operational precipitation profile corrections. *J. Appl. Meteorol.* **34**: 2612–2630.
- Joss J, Gori EG. 1978. Shapes of raindrop size distributions. *J. Appl. Meteorol.* **17**: 1054–1061.
- Joss J, Waldvogel A. 1990. Precipitation measurement and hydrology. Pp 577–597 in *Radar in Meteorology: Battan Memorial and 40th Anniversary Radar Meteorology Conference*. Amer. Meteorol. Soc: Boston
- Hossain, F., Anagnostou, E., Borga, M., and Dinku, T. (2004). “Hydrological model sensitivity to parameter and radar rainfall estimation uncertainty.” *Hydrolog. Process.*, 18(17), 3277–3299.
- Kitchen M. 1995. ‘Estimation of surface precipitation rate from radar using a variational method’. Pp 228–238 in *COST-75 Weather Radar Systems – International Seminar, Brussels 1994* vol. EUR 16 013EN.
- Krajewski WF, Georgakakos KP. 1985. Synthesis of radar rainfall data. *Water Resour. Res.* **21**: 764–768.
- Krajewski, W.F., Smith, J.A., 2002. Radar hydrology : rainfall estimation. *Adv. Water Resour.* 25 (8–12), 1387–1394
- Lardet, P. & Obled, C. (1994) Real-time flood forecasting using a stochastic rainfall generator. *J. Hydrol.* 162, 391-408.
- Lee G-W, Zawadzki I. 2005. Variability of drop size distributions: Time-scale dependence of the variability and its effects on rain estimation. *J. Appl. Meteorol.* **44**: 241–255.
- Lee G, Seed AW, Zawadzki I. 2007. Modeling the variability of drop size distributions in space and time. *J. Appl. Meteorol.* **46**: 742–756
- Ogden, F. L., Garbrechl, J., DeBarry, P. A. & Johnson, L. E. (2001) GIS and distributed watershed models, 11. Modules, interfaces and models. *J. Hydrol. Engng* **6**(6), 515-523.
- Morin, E., Maddox, R., Goodrich, D., and Sorooshian, (2005). “Radar z-r relationship for summer monsoon storms in Arizona.” *Weather Forecast.*, 20(4), 672–679.

- Pellarin T, Delrieu G, Saulnier G-M, Andrieu H, Vignal B, Creutin J-D. 2002. Hydrologic visibility of weather radar systems operating in mountainous regions: Case study for the Ardèche catchment (France). *J. Hydrometeorol.* **3**: 539–555
- Pessoa, M., Bras, R., and Williams, E.(1993). “Use of weather radar for flood forecasting in the Sieve River basin: A sensitivity analysis.” *J. Appl. Meteorol.*, 32, 462–475.
- Saulnier, G. & Datin, R. (2004), 'Analytical solving of a bias in the TOPMODEL framework water balance', *Hydrological Processes* **18**(7), 1195-1218.
- Saulnier, G.M.; Beven, K. ; Obled, Ch. , 1997 : Digital elevation analysis for distributed hydrological modelling: reducing scale dependence in effective hydraulic conductivity values. *Water Resources Research*, **33**, 2097-2101.
- Seed AW. 2003. A dynamic and spatial scaling approach to advection forecasting. *J. Appl. Meteorol.* **42**: 381–388.
- Sharif, H., Ogden, F., Krajewski, W., and Xue, M. 2002. “Numerical simulations of radar rainfall error propagation.” *Water Resour. Res.*, 38(8), 1140.
- Stasinopoulos D., B. Rigby, C. Akantziliotou, 2008 : « Instructions on how to use the GAMLSS package in R. 2nd ed, available at :<http://studweb.north.londonmet.ac.uk/~stasinom/papers/gamlss-manual.pdf>.
- Vieux, B., and Bedient, P. (1998). “Estimation of rainfall for flood prediction from WRS-88d reflectivity: A case study, 17–18 October 1994.” *Weather Forecast.*,13(2), 407–415.
- Winchell, M., Gupta, H., and Sorooshian, S. (1998). “On the simulation of infiltration and saturation-excess runoff using radar-based rainfall estimates: Effects of algorithm uncertainty and pixel aggregation.” *Water Resour. Res.*,34(10), 2655–2670.
- Yuter SE. 2002. Precipitation radar. Pp 1833–1852 in *Encycl. Atmos. Sci.* Holton JR, Curry JA, Pyle JA. (eds.) Academic Press: London
- Zawadzki I. 1982. The quantitative interpretation of weather radar measurements. *Atmos.–Ocean* **20**: 158–180.

APPENDIX

GENERATOR CODE

GENERATION OF THE MULTI - GAUSSIAN PERTURBATION FIELD

```
ns: Simulations
nt: number of time – steps
Nmesh: Dimension of the mesh
D_i: Simulated Delta (German approach)
D_cond: Simulated Delta under conditionings
-----
ns<-c(50)
nt<-dim(res)[1]
Nmesh<-dim(res)[2]
mat_delta<-matrix(nrow=Nmesh, ncol=nt)
mat_DELTA<-matrix(nrow=Nmesh, ncol=nt)
mat_Yr_m<-matrix(nrow=Nmesh, ncol=nt)
DELTA<-matrix(nrow=Nmesh, ncol=nt)
D<-array(NA, c(nt, Nmesh, ns))
D_cond<-array(NA, c(nt, nmesh, ns))

for (i in 1:ns){
  for (j in 1:nt){
    Yr_m<-rnorm(Nmesh,m=0,sd=1)
    mat_delta[,j]<-as.vector(lower_m%*%Yr_m)
  }
  mat_DELTA[,1]<-mat_delta[,1]
  mat_DELTA[,2]<-mat_delta[,2]-vec_a_1*mat_delta[,1]
  for (t in 3:nt){
    mat_DELTA[,t]<-mat_delta[,t] - vec_a_1*mat_delta[,t-1] - vec_a_2*mat_delta[,t-2]
  }
  mean_m<-as.numeric(vec_mean_col)
  DELTA<-vec_U * mat_DELTA
  D_i<- mean_m + DELTA
  D[,i]<-D_i

  D_con <- sd_con*t(DELTA)
  D_condi<-m_cod + D_con
  D_cond[,i]<-D_condi
}
}
```

GENERATION OF THE ENSEMBLE OF PROBABILISTIC PRECIPITATION

```
R<- d
F<-array(NA, c(nt, Nmesh, ns))
  for (i in 1:dim(D)[3]){
    mat_F_i<-(R - D[,i])
    F[,i]<-mat_F_i
  }
  ELIMINATION OF NEGATIVE VALUES
ind_negative<-which(F <= 0)
F[ind_negative]<-0
F_2<-array(F, c(nt, Nmesh, ns))
```